Turkish Journal of Physics

http://journals.tubitak.gov.tr/physics/

Research Article

Turk J Phys
(2018) 42: 125 – 135

doi:10.3906/fiz-1706-2

Permanent magnet motion in a copper tube

Jaroslav FRANEK, Martin ŠOKA*
Institute of Electrical Engineering, Faculty of Electrical Engineering and Information Technology,
Slovak University of Technology in Bratislava, Bratislava, Slovakia

Received: 01.06.2017 • **Accepted/Published Online:** 03.11.2017 • **Final Version:** 26.04.2018

Abstract: This paper deals with the investigation of braking forces induced by eddy currents, which have effects on the permanent magnet moving at a constant speed in the direction of the conductive tube axis. The analysis is based on calculation of an action of a force between the current density, representing the magnet, and the eddy currents. The chosen solution is based on classical electrodynamics and can serve as a guide for the calculation of other cases, where braking forces are created between the moving cell, which is a source of the magnetic field, and a close conductive subject. The obtained results indicate the braking force affecting the magnet and the dependence of this force on the current. The graphical representation of the results shows that the balancing velocity of the magnet fall is inversely proportional to the quadrant of its magnetic moment. This work may be useful for experts in the area of the design of electromagnetic clutches, brakes, and actuators and for university teachers dealing with electrodynamics. Moreover, it can serve as a demonstration of a calculation of the field by vector potential, which is an appropriate quantity used for the description of magnetic fields.

Key words: Magnet movement, eddy currents, braking forces, diffusion equation, vector potential

1. Introduction

In the past 20 years, cheap production of neodymium magnets has emerged. These are characterized by high values of energetic product and remanent magnetic field. The magnets are greatly used in demonstrative experiments, among others in the demonstration of braking force created by eddy currents that occur at the change of the magnetic field in a conductive environment. According to Lenz's law, the induced currents try to prevent the change that has created them. As a consequence, braking forces having effects on the permanent magnet moving near the conductor come into existence.

One of the frequent experiments that has been, for years, a point of interest of many experimental and theoretical studies [1–5] and can be easily executed is the fall of a (neodymium) magnet through a thick-walled (well-conductive) copper tube. The popularity of these experiments is because of their highly demonstrative display. From the previously cited sources [3,4], it follows that the permanent magnet falls through the copper tube during regular experiments in a time that is one or two orders longer than the flyover time of a nonmagnetic object on the same trajectory. In other words, a nonmagnetic object moves with a constant acceleration g (if we do not take the effect of the air into account) and a neodymium magnet after its entry into the copper tube reaches its terminal velocity in a time of less than a few hundredths of a second and then moves at a constant speed [4]. At a constant speed, gravitational and braking forces are in balance.

*Correspondence: martin.soka@stuba.sk

In the present paper, we discuss the determination of the breaking force affecting the magnet that moves at a constant speed in the direction of the axis of the conductive (copper) tube. It is based on classical electrodynamics and the problem is solved under some simplifying assumptions. It is the aforementioned constant speed; therefore, we do not solve the case of accelerated movement and the wave radiation to the surroundings connected with it. We consider the movement to be clearly axial (oriented in the direction of the Z axis) and we do not consider other degrees of mechanical latitude of a falling magnet (such as rotation around its own axis, oscillation, etc.). The wall of the tube is considered to be sufficiently thick and we do not consider the effect of air on the magnet. The basic layout of the experiment, which is described here, is depicted in Figure 1a. The natural coordinate system suitable for the physical description is the cylindrical coordinate system depicted in Figure 1a. Another simplification is the assumption that the diameter of the magnet and the inner diameter are substantially bigger than the air gap between the magnet and the inner wall of the tube. This means that instead of the situation depicted in Figure 1a we can solve the situation depicted in Figure 1b. In Figure 1b, the plain metal–air interface is presented instead of the copper tube and it presents the case where the diameter of the tube is in the limit point to infinity. The natural coordinate system in Figure 1b is the Cartesian coordinate system. The magnet itself falling in the direction of the Z axis parallel to the tube wall is represented by the line density of the current (ideally represented by a thin and infinitely long strip), which induces a magnetic field interfering in the conductive wall. This magnetic field is variable in time due to the magnet's movement and causes eddy currents in the conductor (copper) and consequently a braking effect on the falling magnet. If we consider the situation according to Figure 1b, then when determining the braking force we have to look for the braking force affecting the measurement of the strip length with the current oriented in a direction perpendicular to the layout. The strip is infinitely long; only the force on the measurement of length makes sense.

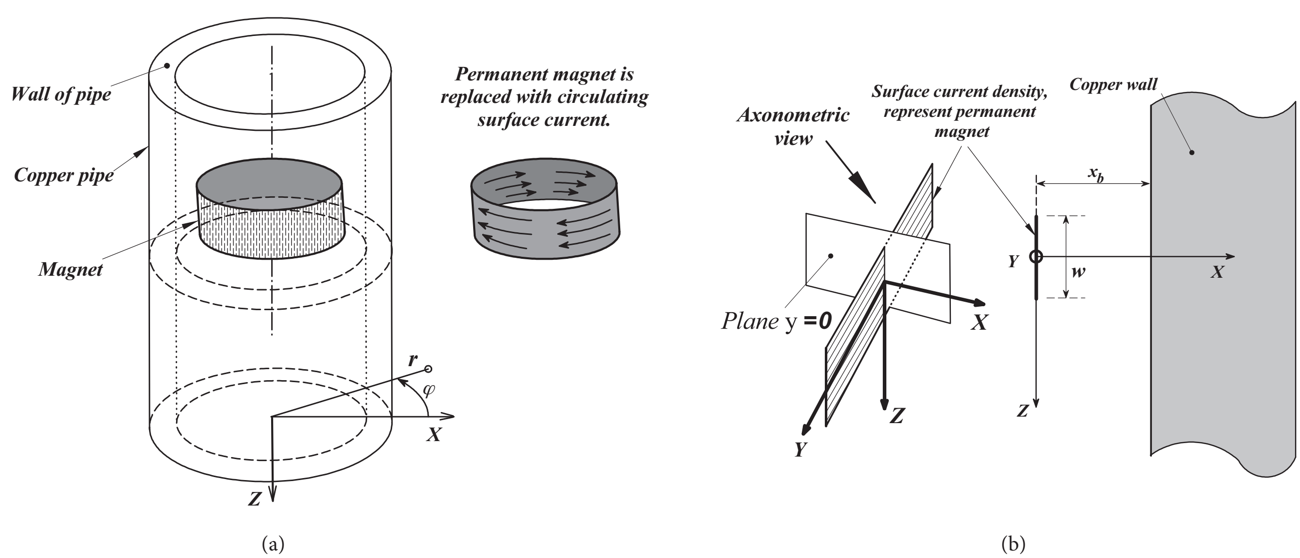

Figure 1. (a) The basic experimental setup. (b) Current strip, with w width, near the copper wall.

2. Theoretical description

2.1. Modeling of a permanent magnet

A permanent magnet is modeled by a current density circulating on the perimeter of the magnet, which corresponds to homogeneous magnetization of its volume. The field is calculated according to the Biot–Savart law. The surface line density of the current is considered as a constant with value $\boldsymbol{M}$. This modeling leads to the same results for the radial as well as for the axial component of the magnetic field of a cylindrical magnet, as stated in [3,5], while the mentioned papers used the dual approach and modeled the permanent magnet as a pair of disks with the same size and the opposite polarity of the magnetic charge. Both approaches (the field source is either surface current $\boldsymbol{M}$ circulating on the surface of the magnet or is square density of magnetic monopoles $\boldsymbol{M}$ on the pole areas of the magnet) are based on the idea of a magnet with a constant value of the magnetization vector $\boldsymbol{M}$ in the whole volume and lead to the same value of the whole dipole moment. The essential thing for the solution of our problem, determining the braking force affecting the magnet, is that the magnetic field of a permanent magnet (with a radial and axial component) determined in this way is going to be considered as a "hard" source of the magnetic field and therefore the edge condition while solving the field inside the wall of the conductive cylinder. In the case according to Figure 1b, we need to calculate the magnetic field (its two components) in the vicinity of an ideally thin and infinitely long strip where the constant density of the surface current flows. In this case the Biot–Savart law can also be applied, or analytic expressions, which can be derived for the case of the thin and long strip.

Considering quantitative values used in simulation, we have to state that neodymium magnets are characterized by a high value of magnetization (typical value $J_m = 1.3$ T) and therefore also the value of the excitation field. We have to proceed according to the stated typical magnetization value while determining the field in the vicinity of the magnet. Either we proceed according to the clearly dipole moment or from a more precise model of two circular discs (b), or the square current of circulating on the magnet perimeter (a).

2.2. Conditional equations derivation

The calculation of braking forces affecting the permanent magnet will gradually be transformed into a calculation according to the vector potential $\boldsymbol{A}$, consequently to the determination of the magnetic field and finally to the determination of the current field of eddy currents in the tube wall. We will determine the braking force as a force acting between the current field creating the magnet and the current field of eddy currents in the tube wall.

The foundation is the known equations expressing the intensity of the electrical and magnetic field by dynamic potentials (vector potential $\boldsymbol{A}$ and scalar potential Θ). When not considering the displacement currents in the metal in comparison with the conduction ones, we can write the following equations:

$$\vec{E} = -\frac{\partial \vec{A}}{\partial t} - grad(\Phi) \qquad \vec{B} = rot(\vec{A}) \tag{1,2}$$

$$rot(\vec{B}) = \mu_0.\vec{J} = \mu_0.\kappa.\vec{E} \tag{3}$$

$$\nabla^2 \vec{A} - \mu_0.\kappa.\frac{\partial \vec{A}}{\partial t} = 0 \tag{4}$$

Eq. (4), also known as the homogeneous diffusion equation, is a special case of the wave equation of the vector potential obtained while not considering displacement currents in the conductor in comparison with the conduction ones (μ_0 and κ are the permeability of the vacuum and conductivity of copper). The edge condition for Eq. (4) will be the magnetic field of the permanent magnet on the inner wall of the conductive tube. It is given by the magnetic field being only insignificantly influenced on the inner wall by the field of eddy currents in the copper volume. In other words, we can consider the permanent magnet to be a "hard" source of magnetic field and, with known parameters of the permanent magnet, it is possible to calculate it (in our case by the Biot–Savart law). The calculated field of magnetic induction is, in accordance with Eq. (2), the rotation of the vector potential for every place on the inner surface of the tube. There are more advantages to this procedure: 1) the vector potential will have only one nonzero component, the component to the direction of the current; 2) if we fulfill the edge condition for one component of the magnetic field, then the second component of the field automatically gives us the correct result, and therefore both components of the magnetic field will be identical with the two components of the magnetic field created on the surface of the conductive wall by a magnet; 3) in the literature the approach to the view of the mentioned components of the magnetic field of the permanent magnet are not unified, i.e. in [1] during the theoretical determination of braking force, they work only with the radial component of the magnetic field, while [6] works with the axial component (in both cited cases, the experiment corresponds with Figure 1a). While describing the magnetic field by vector potential, this "dilemma" does not exist.

Let us make use of the fact that we are dealing with a situation in which the speed of fall $\boldsymbol{v}$ is constant. For the magnet position $z(t)$ in zero initial position, we have:

$$z(t) = v.t \tag{5a}$$

In this case the time derivation can be replaced by a spatial one:

$$\frac{\partial}{\partial t} = \frac{\partial}{\partial z}.\frac{\partial z(t)}{\partial t} = v.\frac{\partial}{\partial z} \tag{5b}$$

When completing Eq. (4) with Eq. (5b), the number of variables in diffusion equation decreases:

$$\nabla^2 \vec{A} - \mu_0.\kappa.v.\frac{\partial \vec{A}}{\partial z} = 0 \tag{6a}$$

We introduce the substitution:

$$\mu_0.\kappa.v = \frac{2}{\Theta} \tag{6b}$$

The θ constant has the dimension of length, and Eq. (6a) gains the following form:

$$\nabla^2 \vec{A} - \frac{2}{\Theta}.\frac{\partial \vec{A}}{\partial z} = 0 \tag{6c}$$

Eq. (6c) can be described in more detail by cylindrical coordinates (Figure 1a) or in Cartesian coordinates (Figure 1b). In the first case, the vector potential will be the function $A_\varphi(r, z)$, and in the second case, function $A_y(x, z)$:

$$\frac{\partial^2 A_y}{\partial x^2} + \frac{\partial^2 A_y}{\partial z^2} = \frac{2}{\Theta}.\frac{\partial A_y}{\partial z} \tag{7}$$

2.3. Solution of the conditional equation and dispersive relations

Eq. (7) can be solved by separation of the variables. We always obtain two separated differential equations:

$$A_y(x,z) = X(x).Z(z) \tag{8}$$

$$\frac{\partial^2 X(x)}{\partial x^2} - \gamma_x^2.X(x) = 0 \tag{9}$$

$$\frac{\partial^2 Z(z)}{\partial z^2} - \frac{2}{\Theta}.\frac{\partial Z(z)}{\partial z} + \gamma_x^2.Z(z) = 0 \tag{10}$$

Let us solve here Eqs. (9) and (10). They are connected by a separation constant γ_x, which can be a complex number. The solution to Eq. (9) is:

$$X(x) = C_1.\exp(-\gamma_x.x) + C_2.\exp(\gamma_x.x) \tag{11}$$

The solution of Eq. (9) in the form of Eq. (11) is composed of two particular solutions, which we label as a direct and a reverse surface wave. C_1 and C_2 are temporarily unidentified constants and the complex number γ_x is interpreted as a complex propagation factor of a wave; its real part is a damping constant and its imaginary part is a phase constant. Eq. (10) as well as Eq. (9) are linear differential equations. Corresponding with the differential equation of Eq. (10) is the characteristic quadratic equation:

$$\xi^2 - \frac{2}{\Theta}.\xi + \gamma_x^2 = 0 \tag{12a}$$

If we define γ_x as a complex propagation factor in the direction of the X axis, then the unknown ξ in Eq. (12a) will represent the complex propagation factor in the direction of the Z axis. Therefore, we introduce the substitution $\xi = \gamma_z$:

$$\gamma_z^2 - \frac{2}{\Theta}.\gamma_z + \gamma_x^2 = 0 \tag{12b}$$

There are two complex propagation factors in Eq. (12b); each of them describes spreading in the direction of its own axis. Since the axes are orthogonal to each other, the following applies for the propagation factors:

$$\gamma_x^2 + \gamma_z^2 = \gamma^2 \tag{13}$$

Here, γ is the known propagation factor of a plane electromagnetic wave in a well-conductive environment:

$$\gamma^2 = j.\omega.\mu_0.\kappa = j.k_z.\frac{2}{\Theta} \tag{14}$$

In Eq. (14), besides the imaginary unit j and the previously mentioned copper conductivity and vacuum permeability, the angular frequency ω and the wave number k_z also appear.

$$k_z = \frac{\omega}{v} = \frac{2.\pi}{L} \tag{15}$$

To define the term of angular frequency and respectively the wave number appearing in Eqs. (14) and (15), we need to introduce a period. We will do it later; now we finish the solution of Eq. (10). After putting Eq. (13) into (12b), we obtain the roots of Eq. (12b):

$$\gamma_{z1} = j.k_z \quad \gamma_{z2} = \frac{2}{\Theta} - j.k_z \tag{16a,16b}$$

The pair of roots of Eqs. (16a,16b) can be expressed more easily, by definition k_θ:

$$k_\Theta = \frac{j}{\Theta} + k_z \tag{17}$$

$$\gamma_{z1} = \frac{1}{\Theta} + j.k_\Theta \quad \gamma_{z2} = \frac{1}{\Theta} - j.k_\Theta \tag{18a,18b}$$

The solution of Eq. (10) will then be:

$$Z(z) = (a.\cos(k_\Theta.z) + b.\sin(k_\Theta.z)).\exp(\frac{z}{\Theta}) \tag{19}$$

Here, a and b are temporarily undefined constants. We should also recall that, according to Eq. (13), we can also assign γ_x to the known values γ_{z1} and γ_{z2} of the propagation factor for the direction Z (Eqs. (16a,16b)) because the same value belongs to both roots of Eqs. (18a,18b):

$$\pm\gamma_x = \pm\sqrt{\gamma_{z1}.\gamma_{z2}} = \pm\sqrt{j.k_z.\left(\frac{2}{\Theta} - j.k_z\right)} = \pm\sqrt{\gamma^2 - \gamma_{z1}^2} \tag{20}$$

2.4. Introduction of edge periodical conditions

As was stated above in connection with Eqs. (14) and (15), we have to define the term of angular frequency and wave number. Our experiment, the crossing of the magnet moving in a copper tube at a constant speed, can be understood as an intermediate phenomenon with an infinitely long period. This one-time intermediate phenomenon can be replaced by a different one periodically repeating itself. In a repeating (periodical) intermediate phenomenon, we consider magnets that fall gradually one after the other so that there is a distance L (Figure 2). The substitution will be proper if the distance between the magnets is big enough, which means that the field of the magnet from the chosen area $\in$ *(-L/2, L/2)* is only insignificantly influenced by the existence of the other magnets. In such a case we can define the spatial "period" L, basic wave number k_z, and angular frequency $\omega = k_z.v$ according to Eq. (15). If we define the wave number and the angular frequency by Eqs. (14)–(18a,18b), then we can consider it to be the definition of the basic wave number (basic harmonic) and define all the stated relations of Eqs. (14)–(18a,18b) also for the higher harmonic:

$$k_{zn} = n.\frac{\omega}{v} = n.\frac{2.\pi}{L} \qquad n = 1, 2, 3..... \tag{21a}$$

$$\gamma_n^2 = j.k_{zn}.\frac{2}{\Theta} \quad \gamma_{xn} = \sqrt{\gamma_n^2 - \gamma_{z1n}^2} \tag{21b,21c}$$

$$\gamma_{z1n} = j.k_{zn} \quad \gamma_{z2n} = \frac{2}{\Theta} - j.k_{zn} \tag{22a,22b}$$

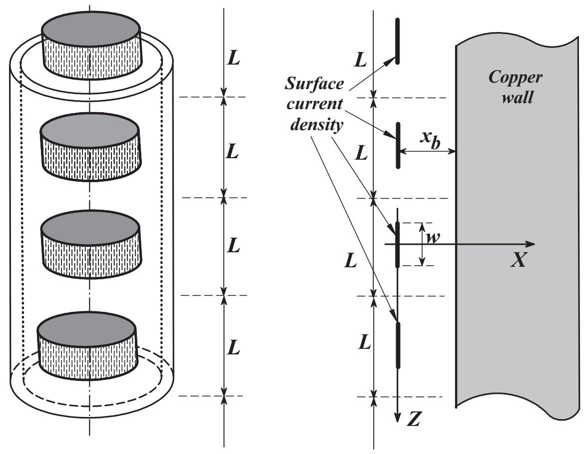

Figure 2. The one-time process replacement by periodical repetition.

$$k_{\Theta n} = \frac{j}{\Theta} + k_{zn} \tag{23}$$

$$\gamma_{z1n} = \frac{1}{\Theta} + j.k_{\Theta n} \quad \gamma_{z2n} = \frac{1}{\Theta} - j.k_{\Theta n} \tag{24a,24b}$$

The solution of Eqs. (9) and (10) can then be written by solution types of Eqs. (11) and (19). In the solution of Eq. (11) we consider only the first element (direct wave), which physically means that we consider the thickness of the tube wall thick enough for the direct wave to cease and not create a back wave. The vector potential (with the orientation in the direction of the Y axis) is expressed in the form of the sum of the infinite series:

$$A_y(x,z) = \sum_n \exp(-\gamma_{xn}.(x-x_b))(a_n.\cos(k_{\Theta n}.z) + b_n.\sin(k_{\Theta n}.z)).\exp(\frac{z}{\Theta}) \tag{25}$$

Here, a_n and b_n are temporarily not defined constants and the significance of the x_b coordinate can be seen in Figure 1b. We have to mention that Eq. (25) as well as other complex terms represent the complex representation of harmonic quantities and their real part is a physical quantity (vector potential) at a given place (x, z).

2.5. Limit point relationships in the case of low speed

Let us notice the previous relationships in the case that velocity $\boldsymbol{v}$ is near zero.

$$\lim_{v\to 0}(\gamma_n) = 0 \quad \lim_{v\to 0}(k_{\Theta n}) = k_{zn} \tag{26a,26b}$$

$$\lim_{v\to 0}(\frac{1}{\Theta}) = 0 \quad \lim_{v\to 0}(\gamma_{xn}) = k_{zn} \tag{26c,2d6}$$

The vector potential given by Eq. (25) in the limit point and for place $x = x_b$ gains the form of the Fourier series:

$$\lim_{v\to 0} A_y(x_b,z) = \sum_n (a_n.\cos(k_{zn}.z) + b_n.\sin(k_{zn}.z)) \tag{26}$$

These coefficients are determined in such a way that it fulfills the periodical edge condition for both assigned components of magnetic field induction $B_x(x_b, z)$ as well as $B_z(x_b, z)$.

Note that according to Eq. (2) the following holds true:

$$B_x(x_b, z) = \frac{-\partial A_y(x_b, z)}{\partial z} \quad B_z(x_b, z) = \frac{\partial A_y(x_b, z)}{\partial x} \tag{28a,28b}$$

We know that the lines of the $\boldsymbol{B}$ vector form closed paths with no known point and it has, in this case, only two nonzero components. The condition of zero divergence in this case can be expressed as:

$$div(\vec{B}) = \frac{\partial B_x}{\partial x} + \frac{\partial B_z}{\partial z} = -\frac{\partial^2 A_y}{\partial x.\partial z} + \frac{\partial^2 A_y}{\partial z.\partial x} = 0$$

It is known that divergenceless of the $\boldsymbol{B}$ field is automatically accomplished by a suitable choice of vector potential. This means that if we chose $\boldsymbol{A}$ so that one of the conditions of Eq. (28) is fulfilled, the second one will be automatically accomplished. As we can see from the previously stated, Eq. (26) is obtained as a result of a limit point, where the speed is declining to zero. The question is: where is the boundary of speed where the limit points of Eqs. (26) and (26) are still valid? The answer is given by Eq. (23), from which we can see that the limit point of Eq. (26b) will be roughly fulfilled if in Eq. (23) we can neglect the imaginary part in comparison with the real one. This condition can be mathematically expressed by introducing critical velocity:

$$v_{crit} = \frac{2}{\mu_0.\kappa.L} \tag{29}$$

The meaning of L (periodical edge conditions) is depicted in Figure 2. Eq. (29) determines the speed border for higher determined relations. These are valid only at speeds lower than the critical velocity determined by Eq. (29). Its value for copper conductivity $\kappa = 5.977.10^7$ S/m and $L =$ 20 cm is $v_{crit} =$13.3 cm/s, which is a larger value than the terminal velocity of a magnet fall as discovered in experiments [3,4,6].

2.6. Determining the current density in metal and the breaking force affecting the magnet

If in Eq. (25) the unknown coefficients a_n and b_n are determined in such a way so that they accomplish the edge conditions, we obtain the expression describing the field of vector $\boldsymbol{A}$. Then we can determine the expression describing the density of the conductive current in the conductor. By filling Eq. (2) into Eq.(3) and by further modification, we get:

$$J_y(x, z) = \sum_n J_y(x, z)_n = -\frac{1}{\mu_0}.\nabla^2 A_y(x, z) = -\frac{1}{\mu_0}\sum_n \gamma_n^2.A_y(x, z)_n \tag{30a}$$

$$A_y(x, z)_n = \exp(-\gamma_{xn}.(x - x_b))(a_n.\cos(k_{\Theta n}.z) + b_n.\sin(k_{\Theta n}.z)).\exp(\frac{z}{\Theta}) \tag{30b}$$

At the known distribution of the current density in metal we can calculate the braking force effects (for a length unit) on the strip so that we first determine the force component for the direction of the Z axis from the force working between the whole strip (1 m long and w wide) and the elementary (differentially small) current flowing through the surface element $dS = dx.dz$ in a perpendicular direction to the layout (Figure 3). This quantity is labeled as the density of the force and its dimension will be in N/m^3:

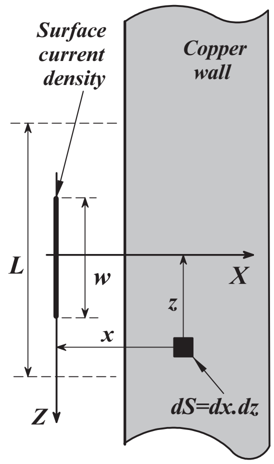

Figure 3. Determining the force affecting the strip.

$$Fp(x,z)_n = \frac{\mu_0.K}{2\pi}.\int\limits_{-\frac{w}{2}}^{\frac{w}{2}} \frac{Re(J_y(x,z)_n).(z-z')}{x^2+(z-z')^2}.dz' \tag{31}$$

The number K is the density of the surface current flowing through the strip and it has dimension A/m. If this force density is integrated through a relevant surface and we add up every element of the set, we get the braking force acting on the length unit of the conductor:

$$F_1 = \sum_n \int\limits_{\frac{-L}{2}}^{\frac{L}{2}} \int\limits_{x_b}^{15x_b} Fp(x,z)_n.dx.dz \tag{32}$$

3. Results, discussion, and comparison with the literature

Results given by Eq. (32) were obtained by a simulation in the math software Mathcad. The dependence of the braking force on 1 m of a strip is carried out for different values of excitation current on the graph (Figure 4a). The graph is on both axes in logarithmic scale and the critical speed is marked there. In values lower than the critical velocity, the dependence is linear, which is in accordance with the results given in [3] and [5]. The deviation of simulated values from the linear dependence occurs in the area of critical speed, where our determined solution of Eqs. (30a, 30b) of the differential equation of Eq. (6a) does not meet the edge condition of Eqs. (28a,28b). We did not consider the modification of the solution for speeds higher than the critical one (Eq. (29)), but it must be noted that the critical speed can be affected by the choice of the L parameter. By reduction of L, the critical speed is increased. However, the negative part is that it affects the magnetic field of the magnet by its virtual neighbors. It is interesting to watch the influence of the excitation current of the strip on the angular coefficient of particular linear dependencies in Figure 4a. This influence is depicted on the graph in Figure 4b, where the size of the excitation current is carried out on the horizontal axis and on the vertical axis, also in logarithmic scale, the angular coefficient of individual dependencies from Figure 4a is carried out. The curve in Figure 4b is in log/log projection linear and corresponds with great precision to the quadratic dependence of unitary force (force per meter) on the size of the excitation current and respectively on the intensity of the magnetic field of the falling magnet. The last statement corresponds with the conclusions of other papers, i.e. in [5] a result where the speed of the magnet fall is indirectly proportionate to the quadrate of the magnetic moment of a falling magnet.

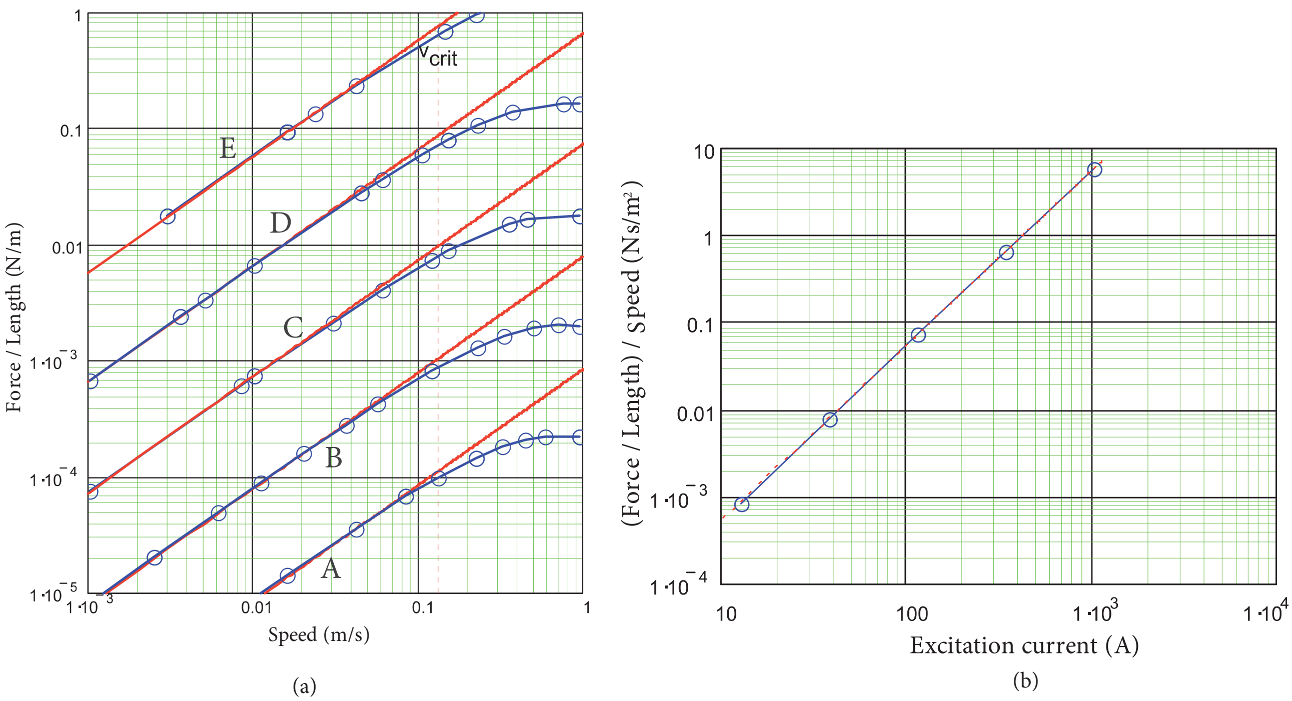

Figure 4. The Mathcad software results. (a) Blue line – simulation, red line – slope of the curve at the beginning, $w =$ 2 cm, $L =$ 20 cm, $x_b =$ 2 mm, $I =$ 12.67 (A), 38 (B), 114 (C), 342 (D), 1024 (E) A. (b) Size of the excitation current dependency of the angular coefficient of individual dependencies from Figure 4a.

It is interesting to notice that a significant number of papers dedicated to the issue of calculation of the braking force affecting the magnet falling in a conductive tube give us results that the authors mark as being in great accordance with the experiment despite the fact that the calculation method is slightly different in these papers. The issue of braking forces calculation is a complex problem that requires simplifications although the physical basis of the inspected phenomenon must be preserved. We assume that the physical basis of the inspected phenomenon should be the consideration of eddy currents as a local parameter, which is determined by solving the corresponding differential equation. Only after that can we introduce integral parameters, which can be, as a rule, expressed and calculated more easily.

Acknowledgments

This work was supported in part by the VEGA Agency of the Slovak Republic (project nos. 1/0405/16 and 1/0571/15) and in part by the Slovak Research and Development Agency (contract nos. APVV-0062-11, APVV-15-0257, and APVV-16-0059).

References

[1] Hahn, K. D.; Johnson, E. M.; Brokken, A.; Baldwin, S. *Am. J. Phys.* **1998**, *66*, 1066-1076.

[2] Weise, K.; Ziolkowski, M.; Carlstedt, M.; Brauer, H.; Toepfer, H. *IEEE T. Magn.* **2015**, *51*, 6201415.

[3] Irvine, B.; Kemnetz, M.; Gangopadhyaya, A.; Ruubel, T. *Am. J. Phys.* **2014**, *82*, 273-279.

[4] Vidaurre, A.; Riera, J.; Monsoriu, J. A.; Giménez, M. H. *Eur. J. Phys.* **2008**, *29*, 335-343.

[5] Levin, Y.; Silveira, F. L.; Rizzato, F. B. *Am. J. Phys.* **2006**, *74*, 815-817.

[6] Knyazev, B. A.; Kotelnikov, I. A.; Tyutin, A. A.; Cherkassky, V. S. *Phys. Uspekhi* **2006**, *49*, 937-946.